Relaxations of Hydrogen-Bonded Liquids Confined in Two-Dimensional Vermiculite Clay

Silvina Cerveny,[†] Johan Mattsson,[‡] Jan Swenson,[†] and Rikard Bergman[†]

Department of Applied Physics, Chalmers University of Technology, SE-412 96 Göteborg, Sweden, and Department of Physics and DEAS, Harvard University, Cambridge, Massachusetts 02138

Received: November 4, 2003; In Final Form: March 17, 2004

Broadband dielectric spectroscopy ($10^{-2}-10^{9}$ Hz) and temperature-modulated differential scanning calorimetry have been performed to study the molecular dynamics of monomer, dimer, and trimer of propylene glycol mono methyl ether (PGME) confined in a two-dimensional layer-structured Na-vermiculite clay. A slight speeding up of the main α relaxation due to the confinement is observed, while the secondary and more local β relaxation is unaffected by the confinement. It was also found that the fragility increased with increasing M_w in both bulk and confined samples. These effects can be attributed to the network formation via hydrogen bonds. We also found indications for a low-dimensional character of the correlation volume involved in the glass transition of PGME and its oligomers.

Introduction

The glass transition (the freezing of a supercooled liquid into an amorphous solid) is a central problem of condensed matter physics, as the mechanism involved is not yet understood.[1] In the past decade the dynamics of molecules close to interfaces,[2,3] in thin films,[4,5] and confined to nanopores[6] has been studied with the aim of increasing the understanding of the glass transition. Of particular interest is to investigate the length scale of cooperative motions near the glass transition. In this study, vermiculite clay is used as a host system which offers a unique possibility to study the dynamic behavior of molecules in a quasi two-dimensional confinement.[7]

The α relaxation process is the main process of dielectric relaxation related to the glass transition of glass-forming materials. Its characteristic relaxation time, τ_α, is essentially proportional to the viscosity and grows as the glass transition temperature, T_g, is approached. τ_α follows a Vogel−Fulcher−Tammann (VFT) behavior:

$$\tau_\alpha = \tau_o \exp\left(\frac{DT_o}{T - T_o}\right) \quad (1)$$

where τ_o is the relaxation time in the high temperature limit, T_o is often identified with the Kauzmann temperature,[8] and D is a parameter which parametrizes the departure from Arrhenius behavior and distinguishes between strong and fragile glasses (high or low D, respectively).[9]

A number of microscopic models have been proposed to explain the non-Arrhenius behavior of the α relaxation. From the classic free volume theory[10−12] to more modern mode coupling approaches[13] cooperative motion is a central concept. Also other models that consider cooperativity have been formulated.[14,15] These models assume that the liquid consists of regions which are dynamically correlated. For example, according to Adam and Gibbs,[15] glass-formers are characterized by a self-organization in the liquid forming cooperatively rearranging regions (CRR). A CRR is defined as a subsystem, which can rearrange into another configuration independently of its environment. In other words, some regions of the sample have to wait for their immediate neighbors to move before they can move. The CRR size can be described by a characteristic length, ξ. This length increases with decreasing temperature until the cooperative region comprises the whole system causing the freezing of mobility at T_o. The characteristic length at T_g of the CRR was estimated to be 1−5 nm in molecular[16−18] and polymer glasses.[19,20] Furthermore, the CRR size has been calculated from different techniques such as calorimetry,[17] dynamic and static light scattering,[21] NMR,[22,23] atomic force microscopy,[24] or dielectric spectroscopy on confined liquids within porous glass.[25] Despite the large number of studies listed above, there is still discussion whether any dynamic heterogeneities exist. It is hoped that the question whether there exists an underlying length scale, which controls the molecular motions responsible for the glass transition, might be answered by investigating the behavior of liquids confined to nanometric scales.

In the present paper we study the finite size effect on the relaxation dynamics of the hydrogen-bonded liquid, propylene glycol mono methyl ether (PGME) and its oligomers using dielectric spectroscopy and differential scanning calorimetry. Dielectric spectroscopy is one of the most powerful experimental tools for studying relaxation dynamics. Recently this method has been used to investigate the dynamics of water,[7] poly(propylene glycol),[26] and molecular glass formers[27] confined in the same vermiculite clay as used in the present study. It has been shown that temperature-modulated dynamic scanning calorimetry (TMDSC) can provide a good estimation of the temperature evolution of the heat capacity $c_p(T)$,[28] which in turn can be used to determine the CRR volume. In this paper we estimate the CRR volume by means of TMDSC and furthermore determine how the glass transition temperature, the temperature dependence of the relaxation time and the shape of the relaxation function is affected by the confinement.

* Corresponding author. E-mail: silvina.cerveny@sw.ehu.es.
[†] Chalmers University of Technology.
[‡] Harvard University.

10.1021/jp037346r CCC: $27.50
Published on Web 07/13/2004

TABLE 1: Characterization of Samples Used in the Present Study[a]

sample	n	M	M_w/M_n	ρ_{bulk} [g cm^{-3}]
PGME	1	90	1	0.937
2PGME	2	148	1	0.951
3PGME	3	206	1	0.956

[a] n denotes the degree of polymerization, ρ_{bulk} is the density, M is the peak molecular weight, and M_w/M_n is a measure of the molecular weight dispersivity.

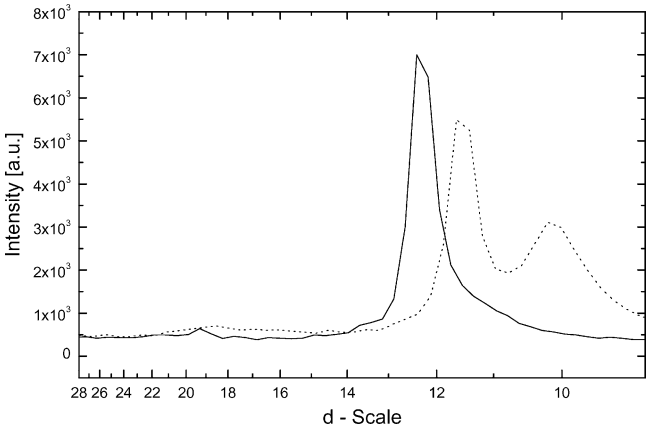

Figure 1. X-ray diffraction data of slightly hydrated Na-vermiculite (dotted line) and when 3PGME was intercalated in the Na-vermiculite (solid line). The scattering angle θ has been converted to a crystallographic d-spacing, as described in the text.

Experimental Section

The monomer, dimer, and trimer of propylene glycol mono methyl ether (PGME) and the dimer of propylene glycol dimethyl ether (PGDE) were purchased from Aldrich Chemical Co. PGME have the chemical formula $OCH_3-(CH_2CHCH_3O)_N-H$ with $N = 1$, 2, and 3, respectively, while for PGDE the formula is $OCH_3-(CH_2CHCH_3O)_N-CH_3$ with $N = 2$. Molecular weights, dispersivity, and density are listed in Table 1. The dimer and trimer were degassed by repeated freeze−dry cycles on a vacuum line. The monomer was desiccated by molecular sieves (3 Å) prior to use.

Vermiculite clay provided by Askania, Sweden, was used as confining host material. The clays were washed and then treated for about six months with 1 M NaCl solution at room temperature, with regular change of the solution, to produce pure Na-vermiculite. Totally dry Na-vermiculite clays were then obtained by drying at 150 °C in a vacuum oven, for 48 h. After drying, the clay pieces were carefully weighed before they were submerged in the respective glass former. The clays were then left in bottles at room temperature for three weeks. Filling was monitored by weighing the samples.

X-ray diffraction was performed to characterize both the filled and unfilled vermiculite clay. In Figure 1 the scattering angle θ has been converted to a d-spacing (the distance between consecutive clay platelets) through the crystallographic relation $d = \lambda/(2 \sin \theta)$, where λ is the wavelength of the incoming X-ray beam). Figure 1 shows the diffraction data for both a slightly hydrated Na-vermiculite (roughly corresponding to one water layer) and a clay fully filled with 3PGME. Two typical d spacings can be observed for the slightly hydrated clay—one at 11.5 Å, which corresponds to water-filled layers, and one at about 10.20 Å, which corresponds to the interplatelet distance for dry Na-vermiculite clay containing only the interlayer Na^+ ions.[29] The d-spacing increases to 12.4 Å when a maximum amount of 3PGME has been intercalated between the clay platelets. This growing in the d spacing is an indication that the liquid is confined between the galleries of the clay system and that the effective layer thickness is about 4 Å (since the diameter of the Na^+ ions is approximately 2 Å).

A broadband and high-resolution dielectric spectrometer, Novocontrol Alpha, was used to measure the complex dielectric function, $\epsilon^*(\omega) = \epsilon'(\omega) - \epsilon''(\omega)$, $\omega = 2\pi f$, in the frequency (f) range from $f = 10^{-2}$ Hz to $f = 10^7$ Hz, and an Agilent RF impedance analyzer 4192B was used for the frequency range 10^6 to 10^9 Hz. The samples were placed between parallel gold-plated electrodes with a diameter of 20 mm and were typically 0.1 mm thick for low frequencies while for the high-frequency setup a smaller cell was used (diameter 10 mm). Isothermal frequency scans of $\epsilon^*(\omega)$ were performed every third degree over the temperature range 130−220 K. The sample temperature was controlled with a stability better than ±0.2 K. It is important to note that the vermiculite clay used in this work was dielectrically neutral, i.e., in the temperature and frequency range of our measurements the dielectric loss of empty clays is negligible.[26]

A DSC Q1000 TA Instrument was used in conventional (DSC) and in temperature modulated (TMDSC) mode. In the DSC mode a cooling−heating cycle between $T_g - 50$ K and $T_g + 50$ K with rates of $|dT/dt| = 20$ K/min was performed using nitrogen as transfer gas. The flow rate used was 50 mL/min. The annealing time between cooling and heating runs was 5 min. From the heat flow/temperature curves, T_g values were calculated as the onset point. Nonhermetic and hermetic aluminum pans were used for confined and bulk materials, respectively.

TMDSC experiments were carried out with a temperature amplitude $T_a = 1$ K. The modulation period was $t_p = 60$ s ($w = 0.105$ rad s^{-1}) and the underlying cooling rate was 2 K/min. The module of the complex heat capacity was calibrated by measuring with sapphire in the studied temperature range and for the frequencies of modulation used in the experiments. In this case, nonhermetic aluminum pans were used for confined and bulk materials, and the flow rate used was 25 mL/min. The sample weights were about 20 mg.

Results

Dielectric Measurements. In time domain the α relaxation of a glass-forming material can normally be described by the Kohlrausch−Williams−Watts (KWW) function[30,31]

$$\phi(t) = \exp\left(-\frac{t}{\tau}\right)^{\beta_{KWW}} \tag{2}$$

where β_{KWW} is the Kohlrausch stretching exponent for the α process. β_{KWW} is between 1 and 0, being unity for exponential relaxation.

Since most dielectric data are collected in the frequency domain, semiempirical frequency-dependent functions are often used to describe the data.[32] The most common is the Havriliak−Negami (HN) expression,[32]

$$\epsilon^*(\omega) = \epsilon_\infty + \frac{\epsilon_o - \epsilon_\infty}{[1 + (i\omega\tau_{HN})^\alpha]^\gamma} \tag{3}$$

where ϵ_o and ϵ_∞ are the unrelaxed and relaxed values of the dielectric constant, respectively, τ_{HN} is the relaxation time, and ω is the angular frequency. In eq 3, α and γ are shape parameters ($0 < \alpha$, $\alpha^*\gamma \leq 1$). It has been shown that for a

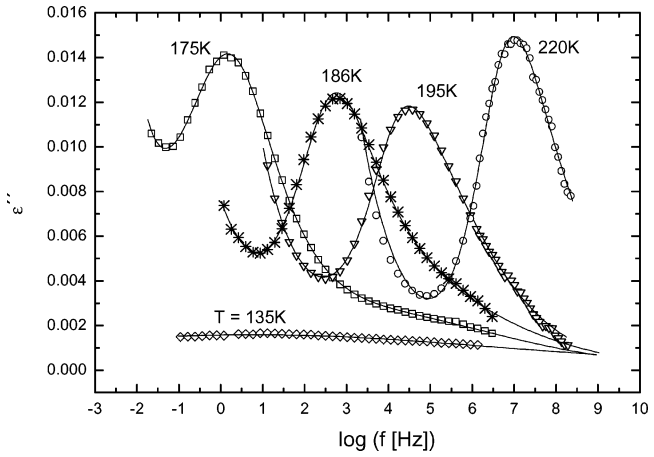

Figure 2. Representative dielectric loss ϵ'' isotherms for 2PGME confined to vermiculite clay. The lines represent least-squares fits to the experimental data.

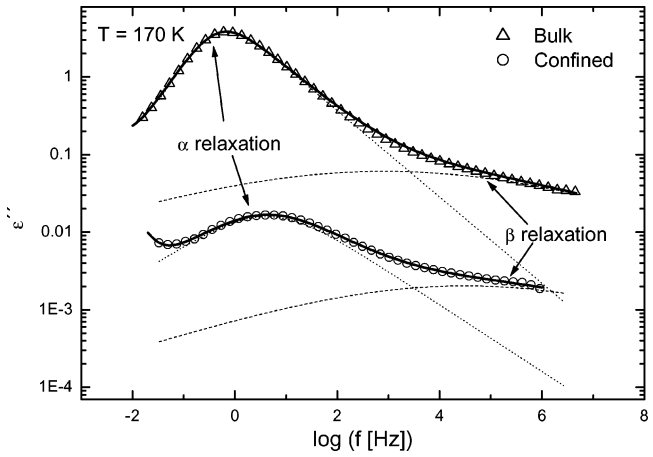

Figure 3. Normalized dielectric loss ϵ'' vs frequency for 2PGME confined in vermiculite clay (circles) and in bulk (triangles). The solid lines are a superposition of eq 4 (dotted line) and the CC function (dashed line).

particular subset of the shape parameters, a good frequency representation of the KWW function can be obtained using eq 3.[33,34] If we set $\gamma = 1$, a symmetrical function[35] is obtained (Cole−Cole function) which is widely used to describe secondary relaxations in glass-forming materials. An asymmetric Cole−Davidson (CD) function is obtained if we set $\alpha = 1$.[36]

Recently, another empirical response function was presented,[37]

$$\epsilon''(\omega) = \frac{\epsilon_p''}{\frac{1-C}{a+b}\left[b\left(\frac{\omega}{\omega_p}\right)^{-a} + a\left(\frac{\omega}{\omega_p}\right)^{b}\right] + C} \qquad (4)$$

where ϵ_p'' and ω_p define the height and position of the peak, while a and b are power-law exponents at the low- and high-frequency side of the peak maximum, respectively. One advantage of eq 4 is that the shape parameters are uncoupled and therefore gives a more stable behavior of the high-frequency b parameter compared to the HN γ parameter. It is important to note that eq 4 includes as a special case the Cole−Cole expression as well as other often-used expressions such as the Fouss−Kirwood[38] and the Jonscher equations.[39]

Isotherms representing the dielectric loss, $\epsilon''(f)$, of the dimer of PGME in clay are shown in Figure 2. Below the glass transition temperature the isotherms present a wide β relaxation whose maximum shifts to higher frequency with increasing temperature. In this temperature range, the low strength of the dielectric loss makes high accuracy measurements in the frequency range above 10^6 Hz difficult. Therefore, below T_g, the reliable frequency range was $10^{-2}-10^6$ Hz. In the vicinity of T_g, isotherms show the α relaxation in the low-frequency range followed by the weaker β process in the high-frequency range. In this temperature range the contributions to the dielectric loss corresponding to the α and β processes are well separated in frequency. Finally, in the neighborhood of 200 K (temperatures well above T_g) both relaxations coalesce into a single peak whose intensity seems to increase with increasing temperature.

In the present study we chose eq 4 with $C = 0$ to fit the α relaxation data for PGME while the β relaxation was described by a Cole−Cole (CC) function for temperatures up to its merging with the α relaxation. Thereafter we used a HN function for describing the β relaxation merged with the α relaxation.

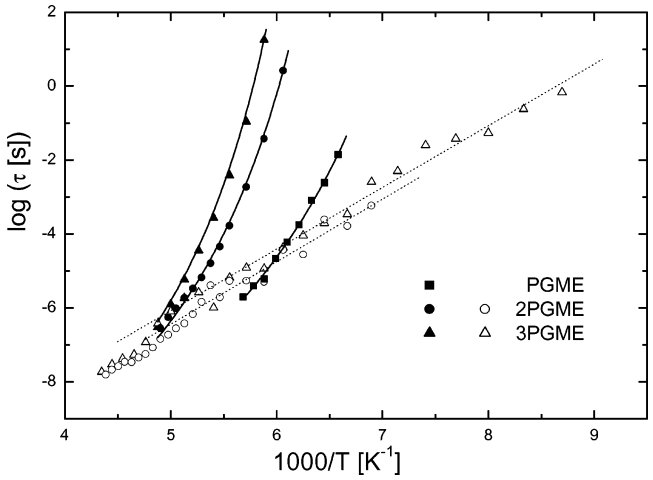

Figure 4. Relaxation times vs inverse temperature for confined PGME. Filled symbols denote the α relaxation, and open symbols represent the β relaxation. The solid lines are fits of the VFT equation to the α relaxation times, and the dotted lines are Arrhenius fits to the β relaxation.

At low frequencies, conductivity effects dominate and to account for that a power law term was added to the sum of eq 4 and the CC or HN function.

Relaxation Times, Shape Parameters, and Dielectric Strength. Isothermal data of the loss peak ϵ'' for confined and bulk PGME at $T = 170$ K are shown in Figure 3. It is clear that the α-peak broadens and shifts to slightly higher frequencies in confinement while the β-peak remains unchanged.

In Figure 4 we show the relaxation times for both α and β processes as obtained from the analysis described above. A direct inspection of this figure shows that the α process becomes faster for shorter chains. The temperature dependence of τ_α can be well described by the VFT equation, eq 1. Extrapolation of this formula to a relaxation time of ∼100 s gives a dielectric estimate of the glass transition temperature, $T_{g,100s}$. This T_g and the VFT parameters describing the temperature dependence of the α relaxation times for bulk and confined samples are given in Table 2.

When discussing the fragility, it is common to use the parameter m, the slope of log τ_α at T_g in an Arrhenius plot, instead of D because the former is well established to correlate with the intermolecular cooperativity of segmental relax-

TABLE 2: Results from Fits to the VFT Equation for the α Relaxation of PGME and PGDE[a]

sample	D	T_o [K]	$\log(\tau_o)$ (s)	$T_{g,100s}$ [K]	m	ΔT_g [K] = $T_{g\ clay} - T_{g\ bulk}$
			Bulk			
PGME	11.2 ± 0.1	109.0 ± 0.1	−13.3 ± 0.1	143.0 ± 0.5	63	
2PGME	9.2 ± 0.1	129.0 ± 0.1	−13.2 ± 0.1	163.0 ± 0.5	73	
3PGME	8.5 ± 0.1	136.0 ± 0.1	−13.2 ± 0.1	169.0 ± 0.5	77	
2PGDE	10.0 ± 0.1	108.0 ± 0.1	−14.9 ± 0.1	136.0 ± 0.5	83	
			Confined			
PGME	9.6 ± 0.3	109.6 ± 0.4	−12.7 ± 0.3	140.9 ± 2.1	68	−2.1
2PGME	6.1 ± 0.3	136.0 ± 0.5	−11.9 ± 0.2	161.7 ± 2.2	79	−1.3
3PGME	5.7 ± 0.3	143.3 ± 0.5	−12.1 ± 0.2	168.5 ± 2.2	85	−1.1
2PGDE	7.8 ± 0.3	112.0 ± 0.5	−14.1 ± 0.1	135.8 ± 2.0	91	−0.2

[a] Bulk data were taken from ref 43.

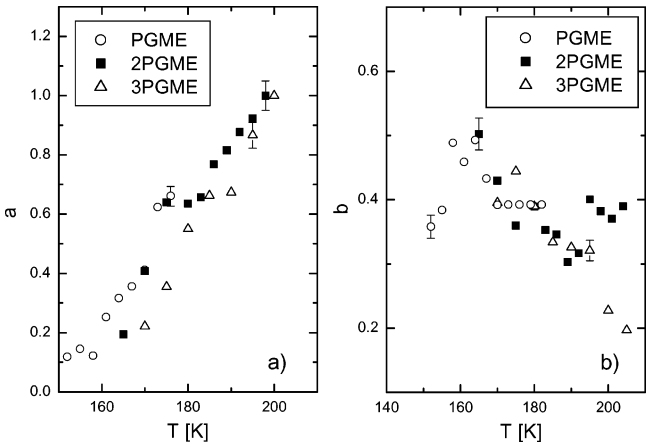

Figure 5. The low- and high-frequency power law exponent, *a* and *b*, from eq 4 for the α relaxation of confined PGME. The error bars are representative for all the values.

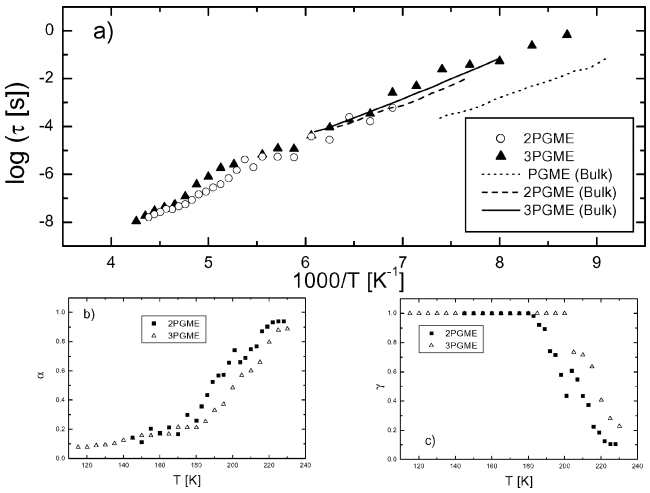

Figure 6. (a) Arrhenius diagram of the β relaxation of PGME confined in vermiculite clay. The lines represent the β relaxation for the bulk material.[43] The error bars are smaller than the size of the symbols. (b) and (c) β relaxation shape parameters vs temperature for confined PGME.

ations.[40,41] In terms of the VFT parameters the fragility is given by[42]

$$m = \frac{DT_o}{T_{g,100s}\ln(10)}\left(1 - \frac{T_o}{T_{g,100s}}\right)^{-2} \qquad (5)$$

The calculated values of *m* are shown in Table 2. It is clear that the fragility increases with increasing molecular weight for both bulk and confined liquids. Similar results were also obtained for PPG confined in the same vermiculite clay.[26]

The shape of the relaxation process is an important characteristic of a glass-former. Figure 5, parts a and b, show the shape parameters *a* and *b* for confined PGME as a function of temperature. For bulk PGME it was found in refs 43 and 44 that $a = 1$ and that *b* is practically independent of temperature. Both *a* and *b* are smaller for the confined samples and *b* is again almost independent of the temperature. In contrast, the parameter *a* has a strong temperature dependence and increases to unity at ∼200 K. In the temperature range between T_g and 1.25 T_g, the main and secondary processes are well separated by at least two decades, allowing a comparison independent of the fitting procedure. In this region, the mean values of parameter *b* are 0.44, 0.39, and 0.35 for the monomer, dimer, and trimer, respectively, which should be compared with the values 0.65, 0.57, and 0.48 for the corresponding bulk samples.[43,44]

Turning to the β relaxation we find that for the confined monomer the dielectric β relaxation loss is too weak to be analyzed. The β relaxation of the dimer and trimer are observable and were found to have an Arrhenius temperature dependence $\tau_\beta(T) = \tau_{\beta\infty}\exp(E_\beta/kT_o)$, where $\tau_{\beta\infty}$ corresponds to a molecular vibration time and E_β is the activation energy that is identifiable with a real energy barrier below T_g. As in the bulk case, all the studied confined liquids have very similar activation energies (0.34 and 0.33 eV for 2PGME and 3PGME, respectively) as shown in Figure 6a. Above T_g, there is a deviation from this Arrhenius dependence. This behavior has been seen for other glass-forming materials and polymers[45−47] and is due to the different temperature dependencies of the α and β relaxation times causing the α and β relaxations to meet at a temperature somewhat above T_g. This region is usually referred to as the "merging region" or the "splitting region". The merging temperature, T_{merg} (here defined as the temperature where both extrapolated relaxation times are the same), was estimated to 204 K and 205 K for 2PGME and 3PGME, respectively. We note that this temperature coincides with the temperature where the *a* parameter of the α relaxation becomes 1. As we mentioned before, we used a linear superposition of CC and eq 4 below T_g and a HN above T_g to fit the overall relaxation spectrum. In the last years a debate has developed about the best way to combine the two relaxation functions, $\phi_\alpha(t)$ and $\phi_\beta(t)$, which describe the α and β relaxation, respectively, for representing the overall relaxation process. Two different approaches have been proposed for analyzing the dielectric response in the merging region: the usual linear superposition[48]

$$\phi(t) = \phi_\alpha(t) + \phi_\beta(t) \qquad (6)$$

which implies a decoupling between the two relaxations and the so-called Williams ansatz[49,50]

$$\phi(t) = A\phi_\alpha(t) + (1 - A)\phi_\alpha(t)\phi_\beta(t) \quad (7)$$

where A is the weight of the α process. In a recent work[46] it has been shown that a relaxation behavior of a series of polymers in the high temperature range, where the main and the secondary relaxation merge, can successfully be described using the two different approaches. In our case, we have chosen for simplicity the simple superposition to fit our data. However, it is important to note that the two ansatzes imply different interpretations of the dynamics at temperatures well above T_g. In particular, the relaxation time of the β relaxation often shows a deviation, as observed here, from the low-temperature Arrhenius behavior. This deviation can be explained using Williams ansatz.[45−47]

In Figure 6b we show the shape parameters, α and γ, for the β relaxation of confined 2PGME and 3PGME. The merging of the α and β relaxations also explains why we observe a crossover from a CC shape of the β relaxation at low temperature to HN ($\gamma < 1$, eq 3) at temperatures close to the merging.

Finally we will analyze the relaxation strength, $\Delta\epsilon$, in the confinement. The absolute value of $\Delta\epsilon$ critically depends on the sample geometry. Since the clay pieces and their distribution in the sample cell are not the same for different samples, it is difficult to determine the absolute value of $\Delta\epsilon$ for confined liquids. Instead of a direct comparison between the bulk and clay system, a relative comparison can be done. For the β relaxation, $\Delta\epsilon_\beta$ was obtained directly from the CC expression. For the α relaxation, we obtained the $\Delta\epsilon_\alpha$ value by numerical integration of the fitted dielectric loss, ϵ''_α, as

$$\Delta\epsilon_\alpha = \frac{2}{\pi}\int_{-\infty}^{\infty} \epsilon''(\omega)\, d(\ln \omega) \quad (8)$$

The ratio between the relative amplitudes between bulk and clay, $((\Delta\epsilon_\alpha/\Delta\epsilon_\beta)_{\text{Bulk}}/(\Delta\epsilon_\alpha/\Delta\epsilon_\beta)_{\text{Clay}})$, is 4.0 ± 0.6 for both 2PGME and 3PGME at $T = 175$ K. It is clear that the relative intensity of the α relaxation is reduced in clay by about a factor of 4. If we assume that the relaxation strength of the β relaxation is basically unaffected by the confinement, this implies that the α relaxation is weaker in the clay than in bulk. A similar change in the relative amplitude of the α process has also been observed for other glass-formers in the same confinement.[26,27]

Heat Capacity Measurements. The TMDSC heating curves for bulk and confined 2PGME are shown in Figure 7. We obtain the absolute heat capacity of confined PGME after subtraction of the absolute heat capacity of the completely dry vermiculite clay. The typical step in the real part of the heat capacity, c'_P, and the peak maximum in the imaginary part c_P'' are observed for bulk as well as confined PGME.

From Figure 7 it is clear that the height of the step of c'_P decreases strongly with the confinement. The same behavior was observed for poly(propylene glycol) confined to nanoporous glasses,[51] but we note that a constant value of the step heat capacity was found for toluene in porous silicates.[52]

Discussion

The molecular dynamics in confined space is determined by surface and finite size effects. In our view the surface effects are due to the chemical interactions between the host systems and the guest molecules, while the finite size effects are related to the restricted length scale on which the underlying molecular fluctuations take place.[53] Surface effects generally cause an increase of the relaxation times (increase of T_g)[2,54] while most studies indicate that finite size effects cause an opposite effect (decrease of T_g).[55,56] The results presented below, strongly suggest that for the confined liquids investigated in this study, the interactions with the walls and the intercalated Na^+ ions must be very weak.

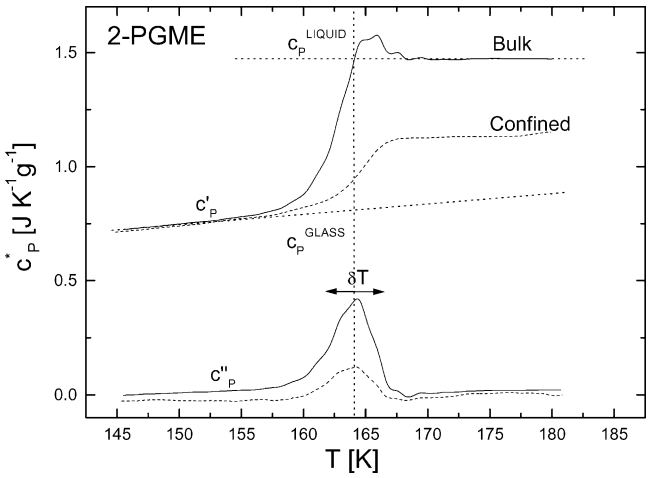

Figure 7. The real part, c'_P, and imaginary part, c''_P, of the complex heat capacity obtained by TMDSC on 2PGME. The solid and dashed lines correspond to the bulk and confined liquids, respectively.

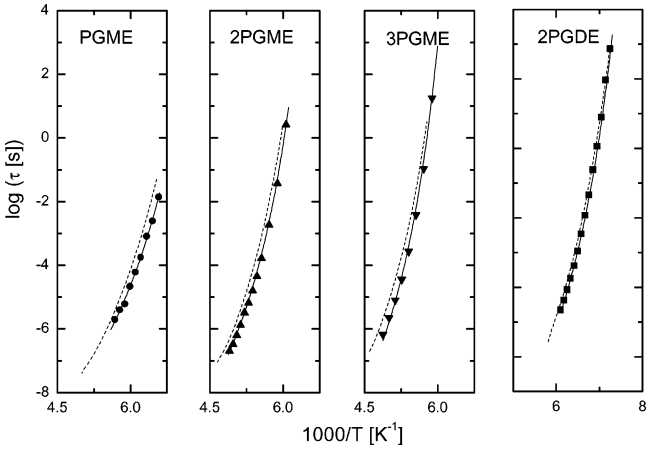

Figure 8. α relaxation time versus inverse temperature for the four studied liquids. Bulk data[43] are presented with dotted lines and confined data with solid symbols. The solid lines are VFT fits to the experimental data points. The error bars are smaller than the size of the symbols.

In Figure 8 we compare the relaxation times, τ_α, of the bulk and confined liquids. Additionally, in Table 2, we show the parameter values obtained from VFT fits shown in Figure 8 for both bulk and confined materials.

As seen in Figure 8, the α relaxation for confined PGME becomes slightly faster compared to the bulk sample. This small increase of the molecular mobility, induced by the 2D confinement, leads to a decrease in the glass transition temperature (here defined as the temperature where the relaxation time reaches 100 s, $T_{g,100s}$) by a few K or less. This negative shift of the glass transition is largest for the monomer $\Delta T_g = -2.1$ K, and the effect decreases with increasing chain length of the glass-former (see ΔT_g in Table 2). This is confirmed by means of DSC. The calorimetric glass transition is shifted by −2.4, −0.5, and −0.3 K for the monomer, dimer, and trimer, respectively. These results can be explained by considering the formation of a H-bonded network. In bulk, the molecules of PGME are able to form transient cross-links between neighboring molecules because of the presence of one terminal OH-

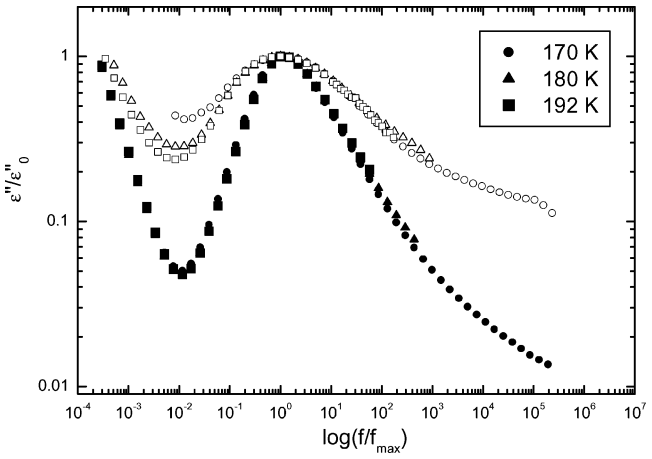

Figure 9. Plots of the normalized dielectric loss against reduced frequency for bulk (filled symbols) and confined (open symbols) 2PGME at the indicated temperatures.

group. Increasing the molecular weight, the density of OH end-groups decreases and the ability to form H-bonding structures decreases. The liquid thus becomes more fragile with increasing molecular weight. When the material is forced to be in a severe confinement (here the interlayer spacing h available for the molecules is about 0.4 nm), the degradation of the H-bonding network becomes stronger than in bulk and speeds up the dynamics (particularly for short chain-lengths where the density of end OH-groups is large). It appears that the confinement affects the network formation such that the liquid becomes more fragile due to the restriction in dimensionality. It is also important to note that the macroscopic density of the confined PGME is lower than that of the bulk PGME, as discussed below. A possible decrease in microscopic density could cause an extra decrease of the number of H-bonds between the molecules.

Additional evidence that the results of the analysis presented above are consistent can be found in the measurements of a non H-bonding glass forming liquid. We chose dipropylene-glycol di-methyl ether (2PGDE) because it has the same monomer unit as 2-PGME, but has no OH end-groups. The procedure to fit the α relaxation was the same as for the samples of PGME. It is clear that the α relaxation time and the dielectric glass transition ($T_{g,100s}$) do not shift compared to the bulk sample, see Figure 8 and Table 2. Also the fragility does not change. We thus conclude that the measured small acceleration in the dynamics of PGME is at least partly due to the degradation of the H-bonding network in the clay. This is also likely to be the reason for the observed increase in fragility.

Confinement-induced negative shifts of the glass transition have been reported, for instance, by Huwe et al.,[57] Zhang et al.,[58] Pissis et al.,[59] and Jackson et al.[55] Huwe et al.[57] studied ethylene glycol (EG) confined in zeolitic systems of different topology. On the basis of dielectric measurements and simulations, they concluded that the number of neighboring molecules decreases from 11 in the bulk liquid to 5 in zeolite β confinement (and further reduction in the channel size decreases the average number of neighboring molecules even more). In that confinement the acceleration of the main relaxation time was dramatic. Although both host systems have a similar nature one should note that in their case the confinement is in all three dimensions, while in our case the geometrical confinement is only in one dimension. Thus, it is evident that the dimensionality of the confinement is of extreme importance for how the dynamics is affected.

Figure 9 shows a log−log plot of the normalized dielectric loss against reduced frequency for bulk and confined PGME. The response becomes broader for the confined liquid and the broadening occurs on both the high- and low-frequency sides. This observation concurs well with the available experimental data on the broadening for other confined molecular liquids,[55,58] confined polymers,[59,60] and polymer films.[61] This behavior thus seems general for all confined materials studied.

For the confined samples, parameter a of the α relaxation tends to approach unity with increasing temperature. This can be interpreted as that the dynamics becomes less and less influenced by the confinement as temperature increases and the length scale of cooperativity decreases. As $a = 1$ corresponds to bulklike dynamics, it is interesting to note that this occurs at temperatures close to the merging of the α and β relaxation which in turn has been related to the onset of cooperativity. This would imply that in our system the starting temperature of the effect of confinement coincides with the onset of cooperativity.

We therefore now focus our attention on the confinement effects on the cooperative dynamics. An estimate of the average volume defining the cooperative rearrangements is possible by measuring the temperature fluctuations in the system:[17]

$$V = \frac{k_B T^2 \Delta(1/c_V)}{\rho \delta T^2} \tag{9}$$

where ρ is the density, k_B the Boltzmann constant, δT the mean temperature fluctuation contribution of the α process related to an average CRR, and $\Delta(1/c_v)$ the step height of the reciprocal heat capacity at constant volume. All the quantities in this equation can be approximately determined from TMDSC.

The method for determining the calorimetric parameters and the characteristic length for the glass transition is shown in Figure 7. The temperature fluctuation values, δT, were obtained from a fit with a Gaussian function to the imaginary part of c^*_p, while $\Delta(1/c_v)$ was approximated by $\Delta c_P/\bar{c}_P^2$ where $\bar{c}_P$ is the average c_P' value between the glass zone and the flow zone, $\bar{c}_p = (c_P^{\text{glass}} + c_P^{\text{liquid}})/2$. c_P^{glass} and c_P^{liquid} values were taken by a tangent construction to the c_P' data (see Figure 7).

Figure 10 shows the dependence of the width of the dispersion δT, the step height Δc_p, and the average volume of the CRR as a function of the molecular weight of the samples of both bulk and confined PGME. The experimental uncertainties of the δT values (±10%) result mainly from the Gaussian fit, and the corresponding for $\Delta(1/c_P)$ (±15%) come from the tangent construction. The accuracy of the average CRR volume is estimated to be 40% for the bulk liquids. On the other hand, the volume in eq 9 also depends on the density. The density of a liquid in confined geometry is difficult to measure and is reported lower than in the bulk for confined liquids in porous glasses.[52,62] In our case, the density of the confined liquid was estimated on the basis of the mass uptake. The results showed that the macroscopic densities of the intercalated oligomers of PGME are lower by around half compared with the density of the bulk. A real density decrease this large is unrealistic. The most likely explanation for the results is that some interplatelet galleries are only partly filled with oligomers of PGME and some layers even remain unfilled, as was even more evident in the diffraction data of propylene glycol and its oligomers intercalated in the same vermiculite clay.[63] The estimate still represents a minimum value for the relevant microscopic density of the confined liquid. In a recent work,[52] it has been shown that the density of confined toluene is quite comparable to that of bulk toluene. On the basis of these results, we chose a microscopic density halfway between the bulk density and the

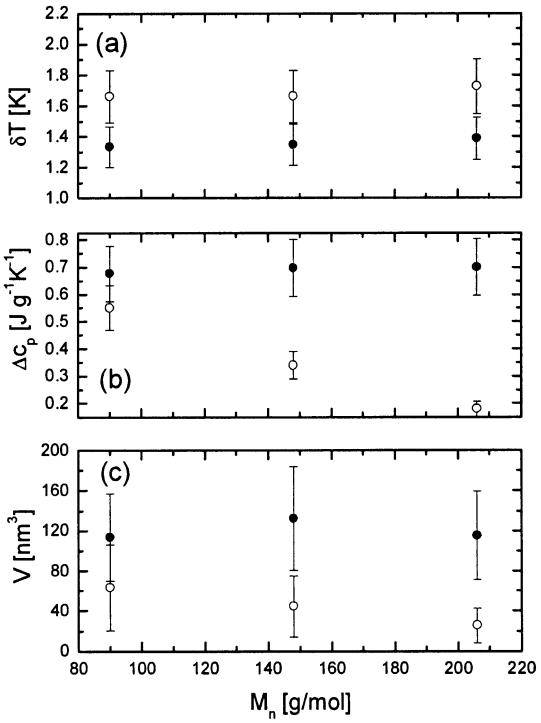

Figure 10. Parameters estimated from TMDSC traces as a function of molecular weight for bulk (filled symbols) and confined (open symbols) PGME. (A) The width of the dispersion δT, (B) the step height Δc_P, and (C) the volume of CRR, V. The uncertainties are discussed in the text.

obtained minimum value, and thus an uncertainty of 33% was assigned for the density of the confined liquid. The resulting uncertainty for the cooperative volume turns out to be approximately 65%, which is a common value for this type of study.[64]

The obtained values of the average CRR volume for bulk PGME and its oligomers, see Figure 10c, are in agreement with the CRR volumes obtained for small glass-forming and hydrogen-bonded molecules such as glycerol, salol, or sorbitol that have been reported[65] to be in the range 100−200 nm^3.

Concerning the parameters estimated from the TMDSC measurements, it is important to note that when a material is confined within a pore (typical size of a few molecular diameters), the characteristic length is not able to extend to distances greater than the pore diameter (cut-off effect). This is not the case in the confined system of this study where the characteristic length is able to grow unlimited in two of the three dimensions.

In Figure 10c, it is evident that the CRR volume decreases in our confinement. However, this decrease is only roughly a factor of 3, which implies that the corresponding characteristic correlation length ξ would be smaller in bulk than in the confinement if we assume that the CRR volume of the bulk liquids has a spherical geometry, i.e., $V = 4\pi\xi^3/3$. This is not a reasonable result considering that the relaxation time is almost unaffected by the present confinement. However, it is not at all obvious what the geometry of a CRR is and how to determine the corresponding correlation length. We thus refrain from such an attempt in this article, although it is clear that a mere assumption of a more flattened CRR would give a more realistic correlation length. This fact in combination with the fact that our confinement gives almost 2-dimensional systems and that we do not find large differences in the relaxation times or T_g's suggests some type of low-dimensional character (<3) of the CRR volume.

Conclusions

We have presented results of the effects of confinement on the dynamics related to the glass transition in the glass-forming liquid propylene glycol mono methyl ether and its oligomers. The main results of the study are

(1) The α relaxation of the confined PGME is slightly faster than in the bulk liquid. This effect decreases with increasing chain length. As a result of the acceleration of the α relaxation, T_g is lower for the confined liquids. The fragility was found to increase with increasing M_w for bulk and confined samples. These results were related to the interplay between confinement and density of hydrogen bonds.

(2) The effect of the confinement is also reflected in the shape of the response that becomes broader for the confined samples. In particular, the broadening of the low-frequency side of the α-peak was found to be strongly temperature-dependent. This implies a connection to the onset of cooperativity as the onset of this low-frequency broadening was found to coincide with the merging of the α and β relaxations.

(3) Our results seem to indicate that the CRR volume of glass-forming liquids is of some type of low-dimensional character.

Acknowledgment. J.S. is a Royal Swedish Academy of Sciences Research Fellow supported by a grant from Kurt and Alice Wallenberg Foundation. J.M. is grateful to the Wenner-Gren Foundations and the Hans Werthen Foundation for support. The Swedish Research Council, Swedish Foundation for Strategic Research and Consejo Nacional de Investigaciones Cientificas y Tecnicas (CONICET- Argentina) are acknowledged for financial support.

References and Notes

(1) Ediger, M. D.; Angell, C. A.; Nagel, S. R. *J. Phys. Chem.* **1996**, *100*, 13200 and references therein.
(2) Schüller, J.; Melnichenko, Y. B.; Richert, R.; Fischer, E. W. *Phys. Rev. Lett.* **1994**, *73*, 2224.
(3) Arndt, M.; Stannarius, R.; Gorbatschow, W.; Kremer, F. *Phys. Rev. E* **1996**, *54*, 5377.
(4) Forrest, J. A.; DalnokiVeress, K.; Stevens, J. R.; Dutcher, J. R. *Phys. Rev. Lett.* **1996**, *77*, 2002.
(5) Forrest, J. A.; DalnokiVeress, K.; Stevens, J. R.; Dutcher, J. R. *Phys. Rev. Lett.* **1996**, *77*, 4108.
(6) Rivillon, S.; Auroy, P.; Deloche, B. *J. Phys. IV* **2000**, *10*, 233.
(7) Bergman, R.; Swenson, J. *Nature* **2000**, *403*, 283.
(8) Vogel, H. *Phys. Z.* **1921**, *22*, 645; Fulcher, G. S. *J. Am. Chem. Soc.* **1925**, *8*, 339; **1925**, *8*, 789.
(9) Böhmer, R.; Ngai, K. L.; Angell, C. A.; Plazek, D. J. *J. Chem. Phys.* **1993**, *99*, 4201.
(10) Cohen, M. H.; Turnbull, D. *J. Chem. Phys.* **1959**, *31*, 1164.
(11) Turnbull, D.; Cohen, M. H. *J. Chem. Phys.* **1961**, *34*, 120.
(12) Turnbull, D.; Cohen, M. H. *J. Chem. Phys.* **1970**, *52*, 3038.
(13) Götze, W.; Sjögren, L. *Rep. Prog. Phys.* **1992**, *55*, 241.
(14) Chamberlin, R. V. *Phys. Rev. B* **1993**, *48* 15638.
(15) Adam, D. G.; Gibbs, J. H. *J. Chem. Phys.* **1965**, *43*, 139.
(16) Fujara, F.; Geil, B.; Sillescu, H.; Fleischer, G. *Phys. B* **1992**, *88*, 195.
(17) Donth, E. *J. Non-Cryst. Solids* **1982**, *53*, 325.
(18) Wagener, A.; Richert, R. *Chem. Phys. Lett.* **1991**, *176*, 329.
(19) Li, K. L.; Jones, A. A.; Inglefield, P. T.; English, A. D. *Macromolecules* **1989**, *22*, 4198.
(20) Heuer, A.; Wilhelm, M.; Zimmermann, H.; Spiess, H. W. *Phys. Rev. Lett.* **1995**, *75*, 2851.
(21) Moynihan, C. T.; Schroeder, J. *J. Non-Cryst. Solids* **1993**, *160*, 52.
(22) Tracht, U.; Wilhelm, M.; Heuer, A.; Feng, H.; Schmidt-Rohr, K.; Spiess, H. W. *Phys. Rev. Lett.* **1998**, *81*, 2727.
(23) Schmidt-Rohr, K.; Spiess, H. W. *Phys. Rev. Lett.* **1991**, *66*, 3020.
(24) Russell, E. V.; Israeloff, N. E.; Walther, L. E.; Gomariz, H. A. *Phys. Rev. Lett.* **1998**, *81*, 1461.
(25) Floudas, G.; Paraskeva, S.; Hadjichristidis, N.; Fytas, G.; Chu, B.; Semenov, A. N. *Chem. Phys.* **1997**, *107*, 5502.
(26) Schwartz, G. A.; Bergman, R.; Swenson, J. *J. Chem. Phys.* **2004**, *120*, 5736.

(27) Bergman, R.; Mattsson, J.; Svanberg, C.; Schwartz, G. A.; Swenson, J. *Europhys. Lett.* **2003**, *64*, 675.
(28) Donth, E. *J. Polym. Sci., Polym. Phys.* **1996**, *34*, 2881.
(29) Skipper, N. T.; Soper, A. K.; Mcconnell, J. D. C. *J. Chem. Phys*. **1991**, *94*, 5751.
(30) Kohlrausch, R. *Ann. Phys.* **1847**, *12*, 393.
(31) Williams, G.; Watts, D. C. T. *Faraday Soc.* **1970**, *66*, 80.
(32) Havriliak, S.; Negami, S. *J. Polym. Sci., Part C* **1966**, *14*, 99.
(33) Alvarez, F.; Alegria, A.; Colmenero, J. *Phys. Rev. B* **1991**, *44*, 7306.
(34) Alvarez, F.; Alegria, A.; Colmenero, J. *Phys. Rev. B* **1993**, *47*, 125.
(35) Cole, R. H.; Cole, K. S. *J. Chem. Phys*. **1942**, *10*, 98.
(36) Davidson, D. W.; Cole, R. H. *J. Chem. Phys.* **1951**, *19*, 1484.
(37) Bergman, R. *J. Appl. Phys.* **2000**, *88*, 1356.
(38) Fouss, R. M.; Kirkwood, J. G. *J. Am. Chem. Soc*. **1941**, *63*, 385.
(39) Jonscher, A. K. *Colloid Polym. Sci.* **1975**, *253*, 231.
(40) Roland, C. M.; Ngai, K. L. *Macromolecules* **1991**, *24*, 5315.
(41) Roland, C. M.; Ngai, K. L. *Macromolecules* **1992**, *25*, 1844.
(42) Ngai, K. L.; Roland, C. M. *Macromolecules* **1993**, *26*, 6824.
(43) Mattsson, J. Ph.D. Thesis, Chalmers University of Technology, Sweden, 2002.
(44) Mattsson, J.; Bergman, R.; Jacobsson, P.; Borjesson, L. To be published.
(45) Bergman, R.; Alvarez, F.; Alegria, A.; Colmenero, J. *J. Chem. Phys.* **1998**, *109*, 7546.
(46) Gomez, D.; Alegria, A.; Arbe, K.; Colmenero, J. *Macromolecules* **2001**, *34*, 503.
(47) Wagner, H.; Richert, R. *J. Phys. Chem. B* **1999**, *103*, 4071.
(48) Garwe, F.; Schönhals, A.; Lockwenz, H.; Beiner, M.; Schroter, K.; Donth, E. *Macromolecules* **1996**, *29*, 247.
(49) Arbe, A.; Richter, D.; Colmenero, J.; Farago, B. *Phys. Rev. E* **1996**, *54*, 3853.
(50) Alvarez, F.; Hoffman, A.; Alegria, A.; Colmenero, J. *J. Chem. Phys.* **1996**, *105*, 432.
(51) Schönhals, A.; Goering, H.; Schick, C. *J. Non-Cryst. Solids* **2002**, *305*, 140.
(52) Morineau, D.; Xia, Y. D.; Alba-Simionesco, C. *J. Chem. Phys.* **2002**, *117*, 8966.
(53) Kremer, F.; Schonhals, A. *Broadband Dielectric Spectroscopy*; Springer: New York, 2003.
(54) Dubochet, J.; Adrian, M.; Teixeira, J.; Alba, C. M.; Kadiyala, R. K.; MacFarlane, D. R.; Angell, C. A. *J. Phys. Chem.* **1984**, *88*, 6727.
(55) Jackson, C. L.; McKenna, G. B. *J. Non-Cryst. Solids* **1991**, *131*−*133*, 221.
(56) Arndt, M.; Stannarius, R.; Groothues, H.; Hempel, E.; Kremer, F. *Phys. Rev. Lett*. **1997**, *79*, 2077.
(57) Huwe, A.; Kremer, F.; Behrens, P.; Schwieger, W. *Phys. Rev. Lett.* **1999**, *82*, 2338.
(58) Zhang, J.; Liu, G.; Jonas, J. *J. Phys. Chem.* **1992**, *96*, 3478.
(59) Pissis, P.; Kyritsis, A.; Daoukaki, D.; Barut, G.; Pelster, R.; Nimtz, G. *J. Phys: Condens. Matter* **1998**, *10*, 6205.
(60) Hall, D. B.; Hooker, J. C.; Torkelson, J. M. *Macromolecules* **1997**, *30*, 667.
(61) Anastasiadis, S. H.; Karatasos, K.; Vlachos, G.; Manias, E.; Giannelis, E. P. *Phys. Rev. Lett.* **2000**, *84*, 915.
(62) Patkowski, A.; Ruths, T.; Fischer, E. W. *Phys. Rev. E* **2003**, *67*, 21501.
(63) Swenson, J.; Howells, W. S. *J. Chem. Phys.* **2002**, *117*, 857.
(64) Hempel, E.; Hempel, G.; Hensel, A.; Schick, C.; Donth, E. *J. Phys. Chem. B* **2000**, *104*, 2460.
(65) Hempel, E.; Huve, A.; Otto, K.; Janowski, F.; Schroter, K.; Donth, E. *Therm. Acta* **1999**, *337*, 163.